International Journal of Modern Physics C
Vol. 24, No. 5 (2013) 1350018 (23 pages)

DOI: 10.1142/S0129183113500186

A SECTION APPROACH TO A TRAFFIC FLOW MODEL ON NETWORKS

ARVIND KUMAR GUPTA

Department of Mathematics, Indian Institute of Technology Ropar, Punjab 140001, India
akgupta@iitrpr.ac.in

Received 16 October 2012
Accepted 10 January 2013
Published 25 April 2013

The development of real time traffic flow models for urban road networks is of paramount importance for the purposes of optimizing and control of traffic flow. Motivated by the modeling of road networks in last decade, this paper proposes a different and simplified approach, known as section approach to model road networks in the framework of macroscopic traffic flow models. For evaluation of the traffic states on a single road, an anisotropic continuum GK-model developed by [Gupta and Katiyar, *J. Phys. A* **38**, 4069 (2005)] is used as a single-section model. This model is applied to a two-section single lane road with points of entry and exits. In place of modeling the effect of off- and on-ramps in the continuity equation, a set of special boundary condition is taken into account to treat the points of entry and exit. A four-section road network comprised of two one-lane roads is also modeled using this methodology. The performances of the section approaches are investigated and obtained results are demonstrated over simulated data for different boundary conditions.

Keywords: Traffic; macroscopic model; section model; network; simulation.

PACS Nos.: 64.60.aq, 47.27.E-,46.15-x.

1. Introduction

As the world's population grows, modeling and simulation methods are becoming essential elements in the design and operation of transportation systems in developing countries like India. Urban streets and their adjacent highways become a continuous traffic flow during rush hours, with vehicles often moving slower than pedestrians. Improving the traffic situation generally involves costly measures that can turn out to be inefficient. Mathematical simulation of traffic flows can help both analyze the existing transport systems and develop new ones.

Nowadays, there exists a broad range of traffic flow models describing the different features and properties of vehicular traffic flow. Roughly speaking, from the level of detail point of view, two types of approaches are commonly used to model vehicular traffic flow: microscopic models e.g. see Refs. 1 and 2 and macroscopic

models e.g. see Refs. 3−12. Microscopic models are based on the supposed mechanisms describing the process of one vehicle following another. In these models, the parameters of interest are the location and the speed of each individual vehicle at each time. On the other hand, macroscopic models are concerned more with the global behavior of traffic stream rather than with interactions between two individual vehicles. In the case of traffic networks, roundabouts and flyovers, drivers have relatively few choices in the paths that they take, so we can achieve an equal amount of control over the flow of traffic with a macroscopic model. Moreover, the data required by a macroscopic model, such as measures of flow and speed, are easily acquired through routine traffic counting, whereas the data for microscopic models is much more difficult to measure and quantify.

The most commonly used macroscopic variables in traffic modeling are the three fundamental traffic parameters: flow-rate, density (or occupancy) and speed. Various theories have been developed to address the problem of estimating the macroscopic traffic parameters in road networks e.g. see Refs. 13−15. Traditionally, continuum models for traffic flow focused on continuous traffic flow on a single road. In continuum mathematical models, vehicular traffic is viewed as a compressible fluid flow, i.e. cars are assimilated to fluid particles, for which suitable balance or conservation laws can be written. Such macroscopic models are often called hydrodynamic or kinematic wave models. The main dependent variables used to describe mathematically the traffic dynamics on stretches of roads are the density of cars $\rho = \rho(x,t)$ and the average velocity $v = v(x,t)$, both at location x and time t. From these quantities, another important traffic parameter is derived: the traffic flow-rate $q = q(x,t)$ given by $\rho * v$ which is of great interest for both theoretical and experimental purposes.

To describe the dynamic properties of traffic on a homogeneous and unidirectional highway, Lighthill and Whitham,[3] and Richards[4] independently proposed a continuum model, which is known as the LWR model in the literature of traffic flow. In this model, a traffic stream model (relationship between fundamental variables: flow, speed and density) is supplemented by the continuity equation of vehicles and the resulting partial differential equation presumably could be solved to obtain the density as a function of space and time. However, besides the continuity equation, one needs an extra dynamic velocity equation in order to describe the emergent traffic jams and stop-and-go traffic. This kind of two-equation model includes Payne−Whitham (PW) model,[5] Kerner−Konhäuser (KK) model,[6] gas-kinetic-based (GKT) model,[16] etc. But, Daganzo[17] pointed out that one characteristic velocity greater than the macroscopic fluid velocity in the two-equation models would lead to nonphysical effects. To overcome this difficulty, Aw and Rascle,[7] Jiang *et al.*[11] and Zhang[12] proposed a second class of higher-order models. Aw and Rascle[7] developed a model to suppress the gas like behavior by replacing the space derivative of density with a convective derivative. Both Jiang *et al.*[11] and Zhang[12] derived a macroscopic equation with anisotropy from car following models. These models are different from

the first class of models in the sense that the anticipation term is a speed gradient (SG) term instead of a density gradient term. Thus, these models are referred to as SG models in the literature of traffic flow. Gupta and Katiyar[9,10] developed an improved anisotropic continuum (GK) model based upon the car following model given by Jiang *et al.*[2] and using the series expansion between headway and density given by Berg *et al.*[8] The qualitative properties and analyses of shock waves and jams are also investigated in their model.[9]

In addition to modeling on single roads first extensions to Lighthill−Whitham[3] traffic flow models on road networks arose in Holden and Risebro,[18] Herty and Klar[19] and Coclite *et al.*[20] The conditions governing the traffic flow through the junction in the network are introduced.[18] They studied traffic waves originating at highway junctions by assuming the existence of an optimization problem at each junction without route choice behavior. But, this model has limited applications in reality. Coclite *et al.*[20] have included the route choice behavior in addition to the idea of solving an optimization problem at each junction. Herty *et al.*[21] extended multiclass LWR model to road networks by proposing criteria for solving Riemann problems at a road intersection. Optimizing criteria for modeling complex traffic intersections like roundabouts by extending two simple cases of merging and diverging is discussed by Herty *et al.*[22] McCrea and Moutari[15] developed a hybrid macroscopic model for traffic flow in road networks. To initiate different traffic flow processes a model of straight road with different boundary conditions is presented as a separate part of the network traffic flow model by Junevičius and Bogdevičius.[23]

Mostly, these approaches are based on the maximization of the flow-rate at the junction to obtain a unique flow-rate value on each road. This approach is complex and not effective in the case of modeling traffic flow for developing countries where most of the junction are congested and have no scope of extension of road lanes. In order to avoid jams near junction, a traffic distribution interchange that provides nonstop and streamlined traffic flow along two crossing routes and that occupies a relatively small amount of land area is being used in major urban centers throughout the world. The construction of flyovers over congested traffic roads, wherever roundabout is not feasible due to space constraint, also helps in reducing the emissions from vehicles and the unnecessary combustion of fuel (petrol/diesel) while waiting for the signal or traffic to clear.

All the above models dominate the field of traffic flow forecasting and real time control on road networks and they are suitable for estimating traffic flow-rate at the locations, on a road network, where loop detectors or sensors are installed e.g. entry/exit of an intersection. However, loop detectors are locally installed and can only make measurements on the vehicles that drive over them. This implies that a closely meshed series of loop detectors is needed to deliver accurate information on the traffic states on a freeway. Because of the higher cost of the installation and maintenance of loop detectors, it is more economical to install less loop detectors and then use an appropriate method to derive the traffic state in less densely equipped areas.

For these purposes, we introduce in this paper a different and simplified approach, known as section approach, which could contribute to simulate effectively traffic flow in road networks. The motivation for achieving a goal of modeling an interchange between two sections of road via boundary conditions is that it would be extremely advantageous to accurately model highway traffic flow while reducing the number of loop detectors used in practice by civil engineers.

In Sec. 2, we present a section approach to model road traffic on roadways and discussed the necessary and sufficient conditions on junctions. To test the validity of the model, we provide the numerical scheme and some hypothetical experiments in Sec. 3. Finally, in Sec. 4, we provide a discussion on our results.

2. Network Flow Model

An urban road network can be composed of links and nodes (intersections, merges and diverges) defining their connection. This study focuses on traffic flow through a highway interchange with the underlying goal of developing and implementing a model that will reduce the number of traffic sensors used in practice. The standard approach of modeling a highway interchange comprised of two one-way roads is to treat the interchange as four individual single lane models and physically measure the traffic density at each boundary of each section using sensors. This would require four sensors at the interchange and four sensors at the boundaries. Alternatively, the approach used in this study incorporates expressions of vehicle flow-rate and momentum flux at the interchange which give boundary conditions at the interchange. Therefore, the density at the interchange can be predicted by the model rather than measured; thus the need for sensors at the interchange is eliminated and only four sensors are enough to control the traffic.

The following sections summarize a fluid-dynamic model describing the traffic dynamics on the freeway part of the network of a road network. We opt for a macroscopic model that yields a sufficiently accurate description of the evolution of the traffic flows for given traffic demands, traffic conditions, and output restrictions on the one hand, and that can be simulated sufficiently fast on the other hand, so that it can be used in on-line traffic control.

2.1. *Model equation for single section*

In this section, we present briefly properties of anisotropic continuum GK model[6] used to describe traffic dynamics at one section when modeling road networks with a continuum type model. In the continuum approach, traffic dynamics in road networks is usually described via the conserved quantities in the model, see e.g. Refs. 18–22.

We consider a homogeneous road section i with constant i.e. time invariant, length L with no entrance or exit ramps. In the case of the GK model,[9] the conserved quantity is the variable $\rho_i = \rho_i(x,t)$, so that on each arc i of the network, the traffic

is governed by the following system of equation:

$$\frac{\partial \rho_i}{\partial t} + \frac{\partial(\rho_i v_i)}{\partial x} = 0, \tag{1}$$

$$\frac{\partial v_i}{\partial t} + v_i \frac{\partial v_i}{\partial x} = \frac{\bar{V}(\rho_i) - v_i}{\tau} + a\,\bar{V}'(\rho)\left[\frac{1}{2\rho_i}\frac{\partial \rho_i}{\partial x} + \frac{1}{6\rho_i^2}\frac{\partial^2 \rho_i}{\partial x^2} - \frac{1}{2\rho_i^3}\left(\frac{\partial \rho_i}{\partial x}\right)^2\right] - 2\beta c(\rho_i)\frac{\partial v_i}{\partial x}, \tag{2}$$

where $\bar{V}'(\rho_i) = \frac{d\bar{V}(\rho_i)}{d\rho_i}$ and $c^2(\rho_i) = -\frac{a\bar{V}'(\rho_i)}{2}$.

These two equations are analogous to the continuity equation and the Navier–Stokes equation, respectively. Here $\rho_i(x,t)$ is the local vehicle density, $v_i(x,t)$ is the local velocity and traffic flow is understood as $q_i(x,t) = \rho_i(x,t)v_i(x,t)$. $\bar{V}(\rho_i)$ is the safe velocity that is achieved in the steady state homogeneous traffic flow. The intrinsic properties on the main highway are prescribed by $\bar{V}(\rho_i)$ and two parameters a and $c(\rho_i)$.

The above system describes a fluid-dynamic approach useful to perform macroscopic phenomena as shock waves formation and propagation.[9] Phase transition of different traffic states are also investigated for the proposed model and the obtained results provide a more accurate description of traffic flow and are consistent with the spectrum of nonlinear dynamic properties reported in the literature.[10]

2.2. *Two-section model*

In order to extend the model for two sections, one needs to define the flow through junctions in the network. Let us consider a long roadway of length $2L$ with one on- and one off-ramps at the middle as shown in the figure.

However, the model (1) and (2) is not sufficient to model a road network since it describes only traffic dynamics along single road section. One way to incorporate the effect of on- and off-ramps is to modified the model (1) and (2) by adding a source or sink terms on the right-hand side of continuity equation.[10] In this paper, the fundamental concept of modeling exit and entrance ramps through boundary conditions is introduced.

The basic idea is to divide the whole road into two single section roads where, the governing equations are exactly the same as the one-section model for both roads as shown in Fig. 1. A vehicle on section 1 now has the option to exit or to continue moving onto section 2. The only new feature is that traffic may enter or exit at the junction through on- and off-ramps. Traffic enters and travels along section 1. As the traffic approaches the junction, some percentage of the traffic will exit while the rest of the traffic will continue onto section 2. Some traffic from another source will enter section 2 at the junction through on-ramp along with the traffic from section 1. In order to incorporate this phenomena, let us introduce a set of distribution coefficient, say a_{ij}, reproducing the behavior of drivers at some junction when choosing an outgoing road section j while coming from an ingoing road section i. Such a set of

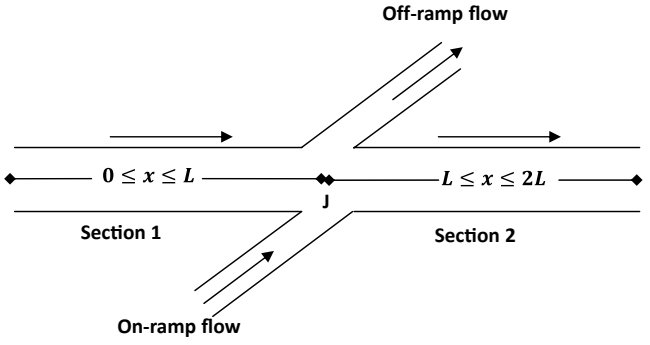

Fig. 1. Sketch of the highway with a single on-ramp and off-ramp.

coefficients give rise, for each junction, to the traffic distribution matrix:

$$A = \{a_{ij}\} \quad \text{where } i, j = 1, 2$$
$$\text{such that } \; 0 \le a_{ij} \le 1 \;\; \forall\, i, j \quad \text{and} \quad \sum_j a_{ij} = 1,$$

where a_{ij} is the probability that a vehicle travels from section i to section j.

The model equations for both sections of road are almost identical to the one-section model equations. With loss of generality, velocity is assumed to be continuous at the interchange, but the density is not necessarily continuous due to the on- and off-ramps. Thus, density must be treated as two separate variables in the model and labeled as $\rho_1(x,t)$ and $\rho_2(x,t)$, respectively.

The governing equations are:

$$\frac{\partial \rho_1}{\partial t} + \frac{\partial (\rho_1 v)}{\partial x} = 0, \tag{3}$$

$$\frac{\partial \rho_2}{\partial t} + \frac{\partial (\rho_2 v)}{\partial x} = 0, \tag{4}$$

$$\frac{\partial v}{\partial t} + v\frac{\partial v}{\partial x} = \frac{\bar{V}(\rho_1) - v}{\tau} + a\,\bar{V}'(\rho_1)\left[\frac{1}{2\rho_1}\frac{\partial \rho_1}{\partial x} + \frac{1}{6\rho_1^2}\frac{\partial^2 \rho_1}{\partial x^2} - \frac{1}{2\rho_1^3}\left(\frac{\partial \rho_1}{\partial x}\right)^2\right] - 2\beta c(\rho_1)\frac{\partial v}{\partial x}, \tag{5}$$

$$\frac{\partial v}{\partial t} + v\frac{\partial v}{\partial x} = \frac{\bar{V}(\rho_2) - v}{\tau} + a\,\bar{V}'(\rho_2)\left[\frac{1}{2\rho_2}\frac{\partial \rho_2}{\partial x} + \frac{1}{6\rho_2^2}\frac{\partial^2 \rho_2}{\partial x^2} - \frac{1}{2\rho_2^3}\left(\frac{\partial \rho_2}{\partial x}\right)^2\right] - 2\beta c(\rho_2)\frac{\partial v}{\partial x}. \tag{6}$$

Here, the domain of the Eqs. (3) and (5) is $0 \le x \le L$ while Eqs. (4) and (6) will be valid on $L \le x \le 2L$. The intrinsic properties on both the section are taken as same.

However, the model (3)−(6) is not sufficient to model a road network since it describes only traffic dynamics along road sections. Therefore, to complete the above model, Eqs. (3)−(6) have to be coupled with some additional formulae modeling the dynamics at intersections and the boundary conditions. As for the boundary conditions, the left boundary of section 1 and the right boundary of section 2 are treated exactly as the boundaries in the one-section model and are given as,

$$\rho_1(0,t) = \tilde{\rho}(t), \quad v_1(0,t) = \bar{V}(\tilde{\rho}(t)), \tag{7}$$

$$\text{At } x = 2L, \quad \frac{\partial^2 \rho_2}{\partial x^2} = 0, \quad \text{and} \quad \frac{\partial^2 v_2}{\partial x^2} = 0, \ \forall\, t \in R_+. \tag{8}$$

Here v_i represents the velocity on the ith section. The left boundary conditions correspond to a specified time-dependent input $\tilde{\rho}(t)$ onto the roadway by assuming that the input density arrives in equilibrium. The outgoing boundary conditions are chosen to allow the traveling wave solution to pass through the boundary without creating any artificial reflections.

In this case, we have only one simple junction comprised of the right boundary of section 1, the left boundary of section 2, the entrance ramp, and the exit ramp. The entrance and exit ramps at the juncture are modeled not as source and sink terms, but rather through a pair of boundary conditions that link the two sections together. The ramps are therefore assumed to exist at the single point $x = L$, and the flow of traffic on the ramps is not explicitly modeled. A natural assumption is the conservation of the flow-rate at intersections. So, the first boundary condition is an expression of the conservation of vehicle flow-rate at the juncture given by,

$$\rho_2(L,t)v_2(L,t) = \rho_1(L,t)v_1(L,t)a_{12} + \rho_{\text{in}}\bar{V}(\rho_{\text{in}}) \quad \forall\, t \in R_+, \tag{9}$$

where ρ_{in} is the traffic density entering from on-ramp at the juncture. This condition is a Kirchhoff-like condition,[24] referred to as the Rankine−Hugoniot condition in conservation law theories. However, the condition (9) does not suffice to determine a unique solution of the system of coupled PDE's to model the flow in the network.[18−23] One needs to define additional conditions at the junction since, we have two unknowns and only one equation at the junction. Existence and uniqueness of solution are guarantee by the following two rules:

(A) The drivers choose roads such that the flux can be maximized, that is we suppose that no car can stop without cross the junction. This entropy condition is derived by maximizing the flux locally at each junction subject to Eq. (9). This condition is automatically satisfied by our assumption of continuity of traffic velocity on the juncture.

(B) The momentum flux at the juncture should be conserved. With analogy to the fluid dynamics, this phenomenon is interpreted as a normal force balance.

$$\mu_1 \frac{\partial v_1(L,t)}{\partial x} = \mu_2 \frac{\partial v_2(L,t)}{\partial x} a_{12} + \mu_{\text{out}} \frac{\partial v_{\text{out}}}{\partial x}, \tag{10}$$

where μ_i is the viscosity coefficient on section i, μ_{out} and v_{out} are the viscosity coefficient and velocity of the traffic on the off-ramp. This seconds boundary condition for our problem will make the system consistent. In terms of traffic flow, this phenomenon can also be interpreted as a drivers memory effect. Equation (10) requires that vehicles which flow onto section 2 along with vehicles that exit "remember" their velocities just before they flow into the juncture. This means that drivers knowledge of their past travel speed has some effect on their future travel speed. Such memory capabilities of human drivers, which assume that drivers flow behavior are based on a "memory window," distributed over the time history of the traffic flow dynamics are also discussed by Sipahi *et al.*[13]

It is worth to mention that under the same homogeneous conditions on both the sections without on- and off-ramps, the two-section model will behave exactly the same as single-section model. The first condition at the juncture i.e. Eq. (9) will be satisfied naturally while the other condition on momentum flux will trivially satisfied as the velocity gradient will vanish at juncture.

2.3. *Four-section model*

In order to provide a nonstop and streamlined flow of freeway traffic, a traffic flow interchange with two crossing routes is discussed. In this section, the idea of two-section model is extended to four one-dimensional sections of road which are linked together at a single node. At the node, a driver has a choice to either continue driving onto the same path or exit onto the other road. The geometrical layout of the interchange of the present investigation can be seen clearly in the plan view of Fig. 2.

The model equations for four sections of road are similar to the two-section model equations. Velocity is assumed to be continuous across the junction between 1 and 2, and across the junction between 3 and 4, but the density is not necessarily continuous due to exiting and entering traffic from different sections. Thus, density must be

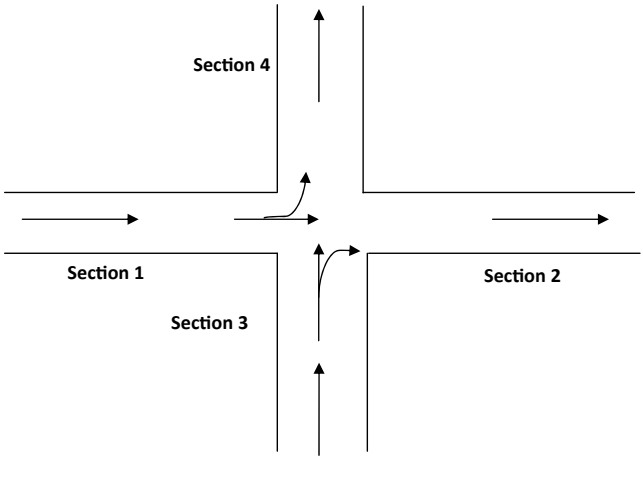

Fig. 2. Sketch of the highway interchange with four sections.

treated as four separate variables in the model and labeled as $\rho_i(x,t)$ for ith section, where $i = 1, 2, 3, 4$.

The governing equations are:

$$\frac{\partial \rho_1}{\partial t} + \frac{\partial(\rho_1 v)}{\partial x} = 0, \tag{11}$$

$$\frac{\partial \rho_2}{\partial t} + \frac{\partial(\rho_2 v)}{\partial x} = 0, \tag{12}$$

$$\frac{\partial \rho_3}{\partial t} + \frac{\partial(\rho_4 v)}{\partial x} = 0, \tag{13}$$

$$\frac{\partial \rho_4}{\partial t} + \frac{\partial(\rho_4 v)}{\partial x} = 0, \tag{14}$$

$$\frac{\partial v}{\partial t} + v\frac{\partial v}{\partial x} = \frac{\bar{V}(\rho_1) - v}{\tau} + a\,\bar{V}'(\rho_1)\left[\frac{1}{2\rho_1}\frac{\partial \rho_1}{\partial x} + \frac{1}{6\rho_1^2}\frac{\partial^2 \rho_1}{\partial x^2} - \frac{1}{2\rho_1^3}\left(\frac{\partial \rho_1}{\partial x}\right)^2\right] - 2\beta c(\rho_1)\frac{\partial v}{\partial x}, \tag{15}$$

$$\frac{\partial v}{\partial t} + v\frac{\partial v}{\partial x} = \frac{\bar{V}(\rho_2) - v}{\tau} + a\,\bar{V}'(\rho_2)\left[\frac{1}{2\rho_2}\frac{\partial \rho_2}{\partial x} + \frac{1}{6\rho_2^2}\frac{\partial^2 \rho_2}{\partial x^2} - \frac{1}{2\rho_2^3}\left(\frac{\partial \rho_2}{\partial x}\right)^2\right] - 2\beta c(\rho_2)\frac{\partial v}{\partial x}, \tag{16}$$

$$\frac{\partial v}{\partial t} + v\frac{\partial v}{\partial x} = \frac{\bar{V}(\rho_3) - v}{\tau} + a\,\bar{V}'(\rho_3)\left[\frac{1}{2\rho_3}\frac{\partial \rho_3}{\partial x} + \frac{1}{6\rho_3^2}\frac{\partial^2 \rho_3}{\partial x^2} - \frac{1}{2\rho_3^3}\left(\frac{\partial \rho_3}{\partial x}\right)^2\right] - 2\beta c(\rho_3)\frac{\partial v}{\partial x}, \tag{17}$$

$$\frac{\partial v}{\partial t} + v\frac{\partial v}{\partial x} = \frac{\bar{V}(\rho_4) - v}{\tau} + a\,\bar{V}'(\rho_4)\left[\frac{1}{2\rho_4}\frac{\partial \rho_4}{\partial x} + \frac{1}{6\rho_4^2}\frac{\partial^2 \rho_4}{\partial x^2} - \frac{1}{2\rho_4^3}\left(\frac{\partial \rho_4}{\partial x}\right)^2\right] - 2\beta c(\rho_4)\frac{\partial v}{\partial x}. \tag{18}$$

Here, the domain of the Eqs. (11), (13), (15) and (17) is $0 \le x \le L$ while Eqs. (12), (14), (16) and (17) will be valid on $L \le x \le 2L$. For simplicity, the intrinsic properties of all the sections are taken as same.

Since the four-section model is a simple extension of two-section model, so the left boundary of section 1 and the right boundary of section 2 are treated exactly as the boundaries in the two-section model. Similarly, the lower boundary of section 3 and the upper boundary of section 4 are treated the same (refer to Fig. 2). However, there is a linkage between all the sections in this case. The linkage is comprised of the right boundary of section 1, the left boundary of section 2, the upper boundary of section 3,

and the lower boundary of section 4. This linkage is also treated in a similar fashion as in the two section case. The coupling conditions are listed below.

$$\rho_2(L,t)v_2(L,t) = \rho_1(L,t)v_1(L,t)a_{12} + \rho_3(L,t)v_3(L,t)a_{34}, \quad \forall\, t \in \mathbb{R}_+, \tag{19}$$

$$\rho_4(L,t)v_4(L,t) = \rho_3(L,t)v_3(L,t)a_{34} + \rho_1(L,t)v_1(L,t)a_{14}, \quad \forall\, t \in \mathbb{R}_+, \tag{20}$$

$$\mu_1 \frac{\partial v_1(L,t)}{\partial x} = \mu_2 \frac{\partial v_2(L,t)}{\partial x} a_{12} + \mu_4 \frac{\partial v_4(L,t)}{\partial x} a_{14}, \quad \forall\, t \in \mathbb{R}_+, \tag{21}$$

$$\mu_3 \frac{\partial v_3(L,t)}{\partial x} = \mu_4 \frac{\partial v_4(L,t)}{\partial x} a_{34} + \mu_2 \frac{\partial v_2(L,t)}{\partial x} a_{32}, \quad \forall\, t \in \mathbb{R}_+. \tag{22}$$

Here v_i represents the velocity on the ith section.

3. Numerical Scheme and Computational Experiments

3.1. *Solution procedure*

In this section, we review the numerical solution method. In doing so, the freeway to be modeled is divided into J nodes and the period of analysis into K time steps. The following difference equations are obtained by applying the finite difference method on the system of Eqs. (1) and (2):

$$\rho_i(j,k+1) = \rho_i(j,k) + \frac{\Delta t}{\Delta x}\rho_i(j,k)[v_i(j,k) - v_i(j+1,k)] + \frac{\Delta t}{\Delta x} v_i(j,k)[\rho_i(j-1,k) - \rho_i(j,k)]. \tag{23}$$

(a) For heavy traffic (i.e. $v_i^j < -2\beta\, c(\rho)$)

$$v_i(j,k+1) = v_i(j,k) + \frac{\Delta t}{\Delta x}(-2\beta c(\rho_i) - v_i(j,k))[v_i(j+1,k) - v_i(j,k)] - \frac{\Delta t}{\tau}(v_i(j,k) - \bar{V}) + \frac{\Delta t}{\tau}\bar{V}'\left[\begin{array}{l} \dfrac{[\rho_i(j-1,k) - \rho_i(j,k)]}{2\,\Delta x\,\rho_i(j,k)} \\ \quad + \dfrac{[\rho_i(j-1,k) - 2\rho_i(j,k) + \rho_i(j+1,k)]}{6\,(\Delta x)^2[\rho_i(j,k)]^2} \\ \quad - \dfrac{[\rho_i(j-1,k) - \rho_i(j,k)]^2}{2\,\Delta x^2[\rho_i(j,k)]^3} \end{array}\right]. \tag{24}$$

(b) For light traffic (i.e. $v_i^j \geq -2\beta\, c(\rho)$)

$$v_i(j,k+1) = v_i(j,k) + \frac{\Delta t}{\Delta x}(-2\beta c(\rho_i) - v_i(j,k))[v_i(j,k) - v_i(j-1,k)] - \frac{\Delta t}{\tau}(v_i(j,k) - \bar{V})$$

$$+\frac{\Delta t}{\tau}\bar{V}'\left[\begin{array}{l}\dfrac{[\rho_i(j-1,k)-\rho_i(j,k)]}{2\,\Delta x\,\rho_i(j,k)}\\ \quad+\dfrac{[\rho_i(j-1,k)-2\rho_i(j,k)+\rho_i(j+1,k)]}{6\,(\Delta x)^2[\rho_i(j,k)]^2}\\ \quad-\dfrac{[\rho_i(j-1,k)-\rho_i(j,k)]^2}{2\,\Delta x^2\,[\rho_i(j,k)]^3}\end{array}\right], \tag{25}$$

where index $j \in J$ represents the road section and index $k \in K$ represents time. Here Δt and Δx are the grid sizes of the finite difference mesh in time and space dimensions, respectively. These equations give the density and velocity value of the ith section at the jth node at time step $k+1$ from the known value obtained at the previous time step k. For the discretization of the conservation Eq. (1), the difference format suitable for physical sense of traffic flow is applied. For the motion Eq. (2) upwind scheme is used. The above difference scheme is suitable for the traffic flow as it maintain the physical properties of the traffic flow even under the extreme conditions.[9]

However, for the linkage node discretization of the modeled equations together with the boundary conditions at juncture are treated in a physical manner. Now, we are explaining the idea of evaluating the unknown at junction in our two-section model. The same concept is extended to compute the variables at junction in four-section model.

Here, at the linking point i.e. $x = L$ (see Fig. 3), the unknown four variables are $\rho_1(n,k+1)$, $\rho_2(1,k+1)$, $v_1(n,k+1)$ and $v_2(1,k+1)$. All the other point except the linkage point is determined by using the algorithm discussed in the previous section. To compute $\rho_1(n,k+1)$, the governing equation of density for section 1, i.e. (3), is discretized at the linkage point using central difference.

$$\begin{aligned}\rho_1(n,k+1) = \rho_1(n,k) - \frac{\Delta t}{2\Delta x}[&\rho_2(2,k+1)v_2(2,k+1)\\ &-\rho_1(n-1,k+1)v_1(n-1,k+1)].\end{aligned} \tag{26}$$

The following discretization is used for Eqs. (9) and (10).

$$\rho_2(1,k+1)v_2(1,k+1) = \rho_1(n,k+1)v_1(n,k+1)a_{12} + \rho_{\text{in}}\bar{V}(\rho_{\text{in}}) \quad \forall\, t \in \mathbb{R}_+, \tag{27}$$

$$\begin{aligned}\mu_1\left[\frac{v_1(n,k+1)-v_1(n-1,k+1)}{\Delta x}\right] = \mu_2&\left[\frac{v_2(2,k+1)-v_2(1,k+1)}{\Delta x}\right]a_{12}\\ &+\mu_{\text{out}}\left[\frac{\bar{V}(\rho_1(n,k+1))-v_1(n,k+1)}{\Delta x}\right].\end{aligned} \tag{28}$$

Due to the assumption of continuity of velocity at the interchange, the system become consistent and the remaining three unknowns orderly can be computed using system of equations comprised of (27) and (28).

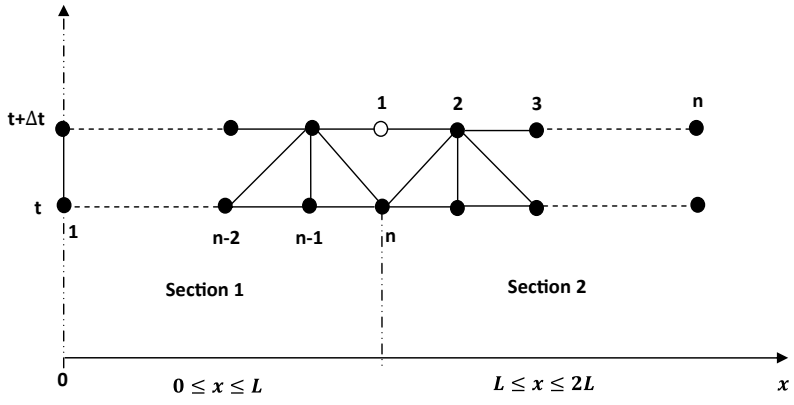

Fig. 3. Uniform grid structure of two-section problem.

3.2. *Numerical experiments*

To better understand the performance of our technique, in this section, we illustrate the results of previous section with some numerical examples. The results on the single section is already tested and presented in Refs. 9 and 10.

3.2.1. *Two-section model*

In order to test the applicability of the two-section model, macroscopic simulation is presented using a hypothetical road of 1.0 km long. Since, two sections are being linked together at a junction in the middle; the total length of each section is taken as 0.5 km. The goal of these simulations is to predict the basic features encountered when two sections of roadway are linked together given an input density and density entering and exiting at the junction. Let us consider the behavior of a localized perturbation, which at time $t = 0$, occurs in an initial homogeneous state of traffic flow and is given by

$$\rho(x,0) = \rho_h + \delta(e^{-\epsilon(x-0.15)^2}), \quad \forall\, x \in [0,1], \tag{29}$$

$$v(x,0) = \bar{V}(x,0), \quad \forall\, x \in [0,1], \tag{30}$$

where ρ_h is the homogeneous density and δ and ϵ are the amplitude and shape parameter of the perturbation.

Assuming that the input density arrives in equilibrium, the left boundary condition of section 1 corresponds to a specified input density $\hat{\rho}$ onto the roadway. To identify the basic features encountered when a section of high density traffic enters the roadway, we take the following boundary condition at $x = 0$.

$$\hat{\rho}(0,t) = \rho_h + \omega(e^{-(t-4)^2}), \quad \forall\, t \in \mathbb{R}_+. \tag{31}$$

In order to allow the traveling wave solution to pass through the boundary without creating any artificial reflections, the right boundary of section 2 is taken as a free outflow (Neumann boundary condition).

For equilibrium speed-density relationship, we use the following relation proposed by Kerner and Konhäuser.[6]

$$\bar{V}(\rho) = u_f \left[\left(1 + \exp\left(\frac{\frac{\rho}{\rho_m} - 0.25}{0.06} \right) \right)^{-1} - 3.72 \times 10^{-6} \right]. \tag{32}$$

For computational purpose, the space domain is divided into equal intervals of length 5.0 m and time interval is chosen as 0.1 s.

The related parameters of our model are as follows:

$$\begin{gathered} \beta = 2.0, \quad \mu_f = 30\,\text{m/s}, \quad \tau = 1.0\,\text{s}, \quad \rho_m = 0.2\,\text{veh/m}, \quad \omega = 0.02, \\ \epsilon = 0.001, \quad \delta = 0.01, \quad \mu_1 = 1.0\,\text{veh-m/s}, \quad \mu_2 = 1.0\,\text{veh-m/s}, \\ \mu_{\text{out}} = 1.0\,\text{veh-m/s}, \quad \rho_h = 0.03\,\text{veh/m}. \end{gathered} \tag{33}$$

Figure 4 depicts the waves that develop from the initial condition (29) and (30), when a small percentage (20%) of traffic on section 1 exits at the junction. For the simplicity, the entrance ramp is kept turn off. In Figs. 4(a) and 4(b), the early time behavior of traffic density and velocity on the roadway are shown. The initial cluster of traffic on section 1 spreads as the traffic flow density is very low and the perturbation decreases its amplitude with time. The same behavior is also discussed on single-section model give by Gupta and Katiyar.[9] At junction, for early time traffic density slightly decreases due to the exiting traffic from off-ramp. It allows a slight increase in the velocity near the junction. As time increases, it is clear from the Figs. 4(c) and 4(d) that the initial cluster spreads and moves towards junction. Finally, when it reaches at the junction, cluster disperses more quickly due to the low density region created by off-ramp. On the downstream side of the junction i.e. the section 2, the low density region is sustained as a result of the continuous exiting of traffic at junction.

To observe the effect of on-ramp, a small constant density of order 0.0045 veh/m is allowed to enter at junction while keeping the exit ramp turned off i.e. $a_{12} = 1.0$ and the results are presented in Fig. 5. It can be viewed from the early time behavior of traffic density and velocity shown in Figs. 5(a) and 5(b) that the initial cluster of traffic centered at $x = 150$ m spreads in the same fashion as in the previous case. The density at junction slightly increases due to the constant continuous entering of vehicle from on-ramp and leads to a slight decrease in the velocity. After 10 s, due to the entering density form the left boundary of section 1, a dipole-like structure is formed as illustrated by Fig. 5(c) in which a complex localized structure of two clusters forms. As time passes, this cluster of traffic spreads and causes an increase in density which leads to a decrease in velocity. After some time, both the clusters merge into a single cluster having a definite shape. It can easily be shown from the figure that as time increases, maximum value of density within the cluster decreases. Figures 5(c) and 5(d) explain that the high density traffic at junction observes a lower density region ahead and speeds up, therefore, the density starts decreasing after the junction. After $t = 60$ s, the density on section 1 becomes homogeneous as the initial cluster and input density

completely passed through the junction. The traffic following the junction continues to speed up in the same manner and therefore, become less dense.

Therefore, for both the experiments, it may be reasonable to conclude that the new model provides a more accurate description of traffic flow and results obtained are consistent with the spectrum of nonlinear dynamic properties reported in the literature.

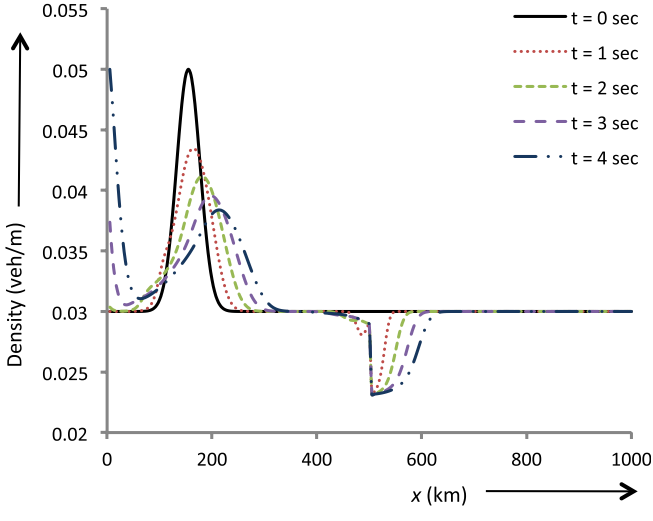

(a)

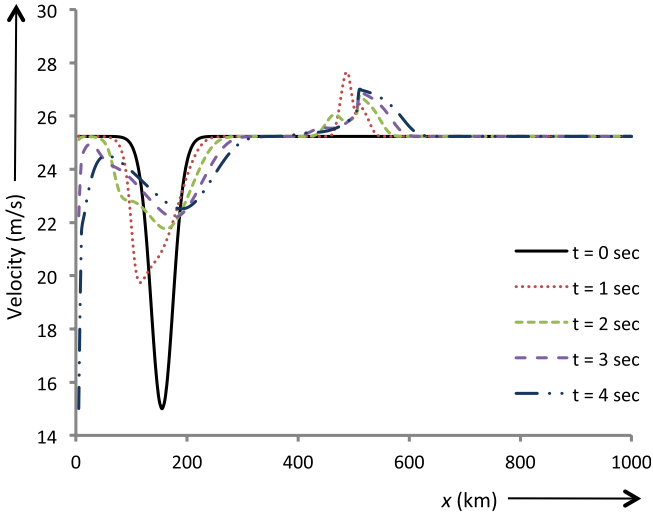

(b)

Fig. 4. (Color online) Evolution of traffic characteristics for two-section model when only entrance ramp is off with $a_{12} = 0.8$. (a) and (c) represent the early and late time behavior of traffic density, respectively. (b) and (d) denote the early and late time behavior of traffic velocity, respectively.

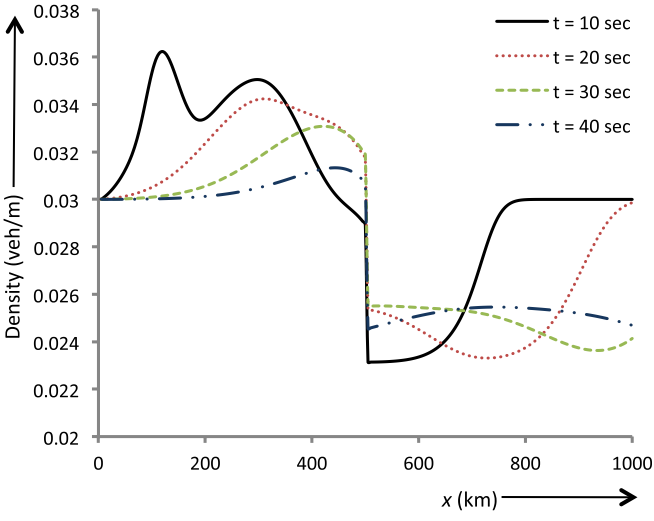

(c)

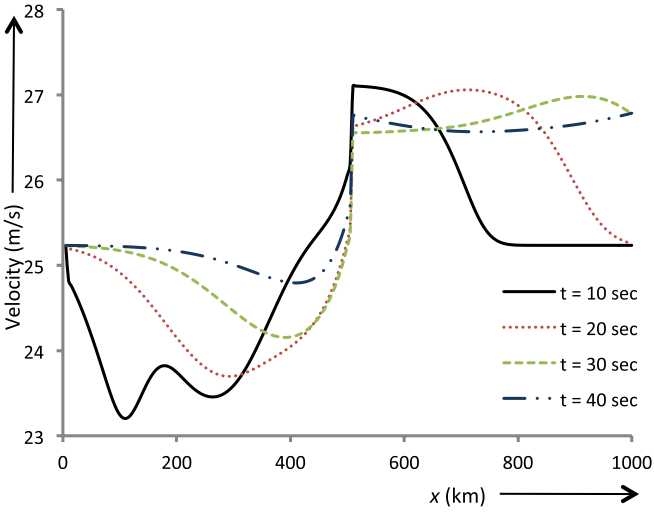

(d)

Fig. 4. (*Continued*)

3.2.2 *Four-section model*

To simulate traffic on the four-section model, we consider two roads each comprised of two sections of roadway 0.5 km long which are linked together at a common node as shown in Fig. 2. It is clear from the figure that the whole highway interchange

is comprised of four sections of roadway which make up two intersecting roads (A and B) of length 1.0 km. Each road is discretized in the same fashion as in the two-section model. The aim of this simulation is to analyze the basic features encountered when two roads are linked together with different input densities and

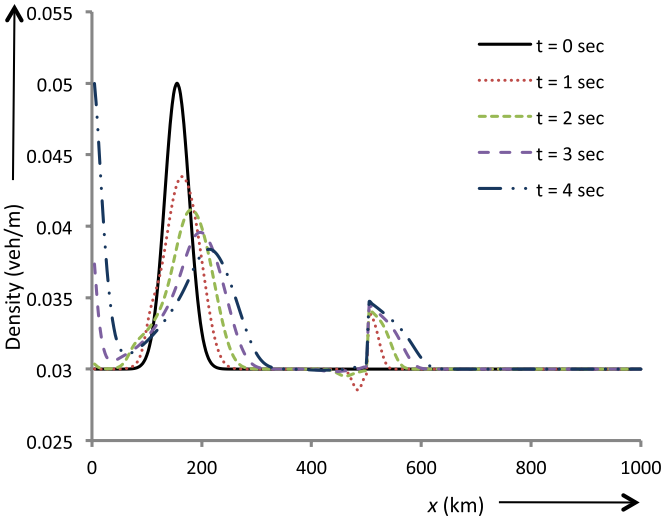

(a)

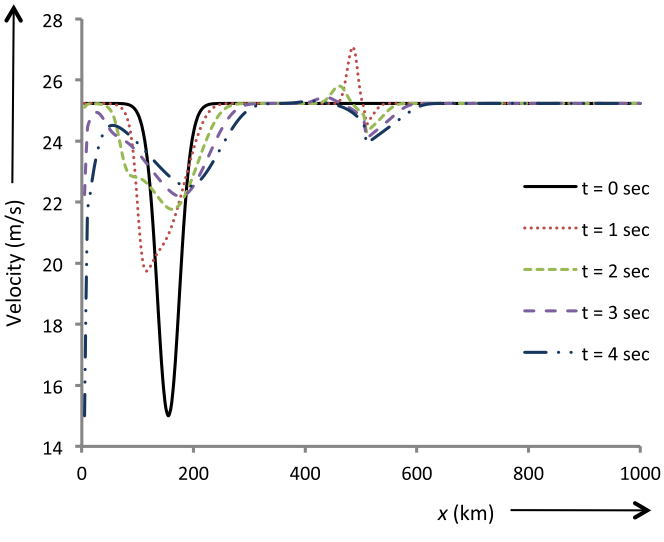

(b)

Fig. 5. (Color online) Evolution of traffic characteristics for two-section model when exit ramp is off and a small constant density 0.0045 veh/m is entering from on-ramp. (a) and (c) represent the early and late time behavior of traffic stream density, respectively. (b) and (d) denote the early and late time behavior of traffic stream velocity, respectively.

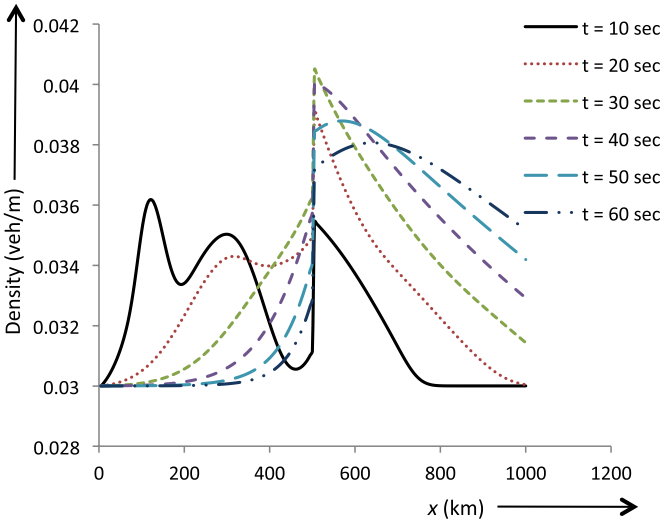

(c)

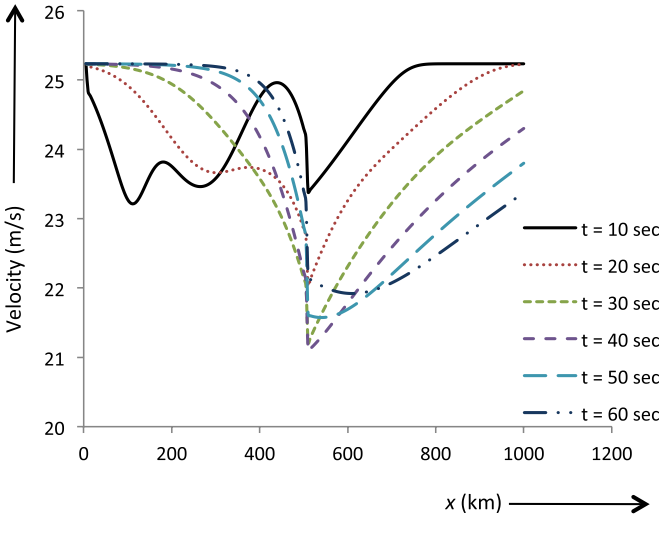

(d)

Fig. 5. (*Continued*)

different initial conditions one each road. The initial density profile on road the roads are kept constant and are given by

$$\rho_A(x,0) = 0.2\,\text{veh/m}, \quad \rho_B(x,0) = 0.24\,\text{veh/m}, \ \ \forall\, x \in [0,1], \tag{34}$$

$$v_A(x,0) = \bar{V}_A(x,0), \quad v_B(x,0) = \bar{V}_B(x,0), \ \ \forall\, x \in [0,1]. \tag{35}$$

The free boundary conditions are taken on the right side of both the roads while, for the left boundary, the following form of input density is taken.

$$\widehat{\rho_A}(0,t) = \rho_h + \omega_A(e^{-(t-4)^2}) \quad \forall\, t \in \mathbb{R}_+, \tag{36}$$

$$\widehat{\rho_B}(0,t) = \rho_h + \omega_B(e^{-(t-7)^2}) \quad \forall\, t \in \mathbb{R}_+. \tag{37}$$

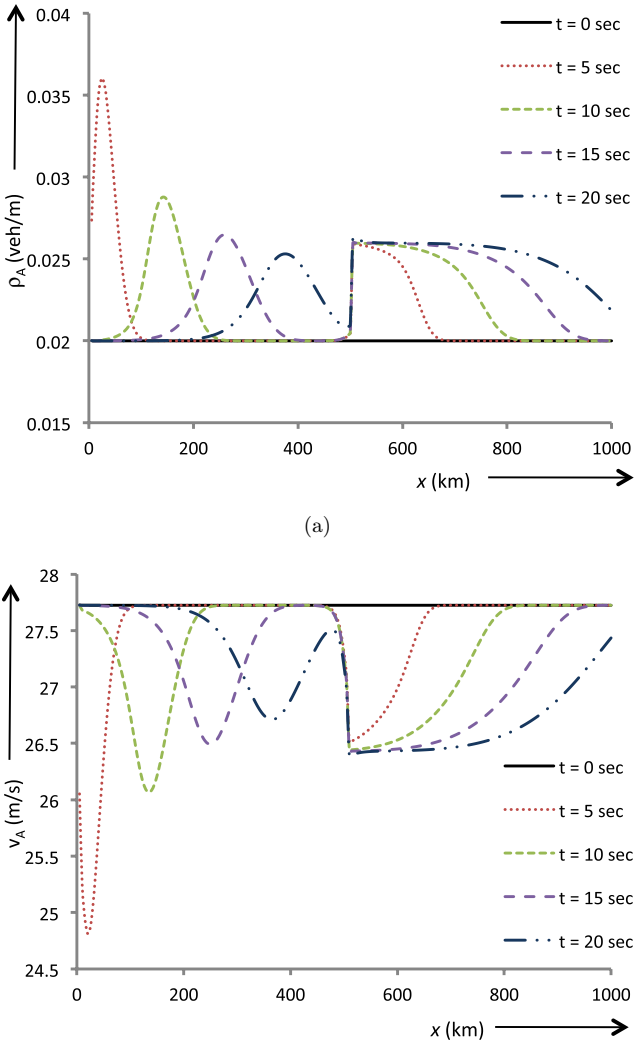

Fig. 6. (Color online) Evolution of traffic characteristics for four-section model: early time effect. (a) and (c) represent the density profile on road A and B, respectively while (b) and (d) show the velocity profile on road A and B, respectively.

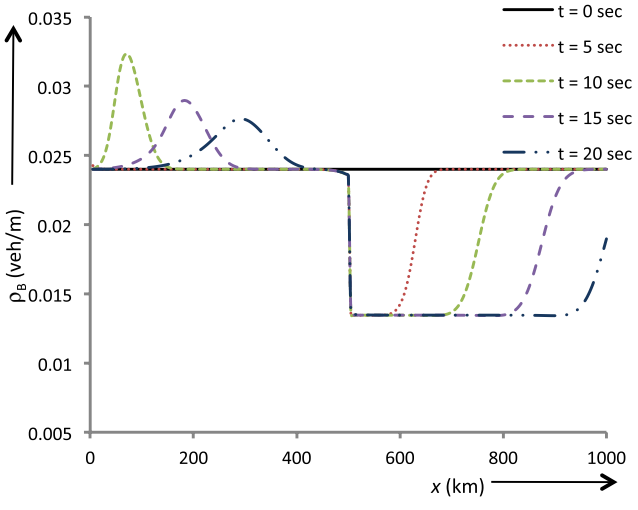

(c)

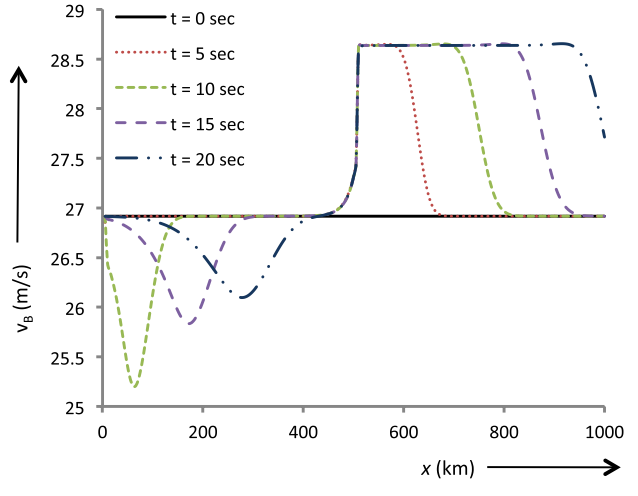

(d)

Fig. 6. (*Continued*)

The following are the parameter used in this study.

$$\beta = 2.0, \quad \mu_f = 30\,\text{m/s}, \quad \tau = 1.0\,\text{s}, \quad \rho_m = 0.2\,\text{veh/m}, \quad \omega = 0.02,$$
$$\epsilon = 0.001, \quad \delta = 0.01, \quad a_{12} = 0.8, \quad a_{34} = 0.4, \quad \mu_1 = 1.0\,\text{veh-m/s}, \tag{38}$$
$$\mu_2 = 1.0\,\text{veh-m/s}, \quad \mu_{\text{out}} = 1.0\,\text{veh-m/s}.$$

The results from the analysis are shown in Figs. 6 and 7. Figure 6 shows the early time behavior of traffic density and velocity on both the roads. Since, both the roads

are at constant density, there are no fluctuations on the roads initially. A cluster starts building on the left boundary of both the roads due to the input densities. Due to the distribution of traffic at interchange, on road A 80% of the traffic from section 1 continues to travel onto section 2 and on road B, 40% of the traffic from

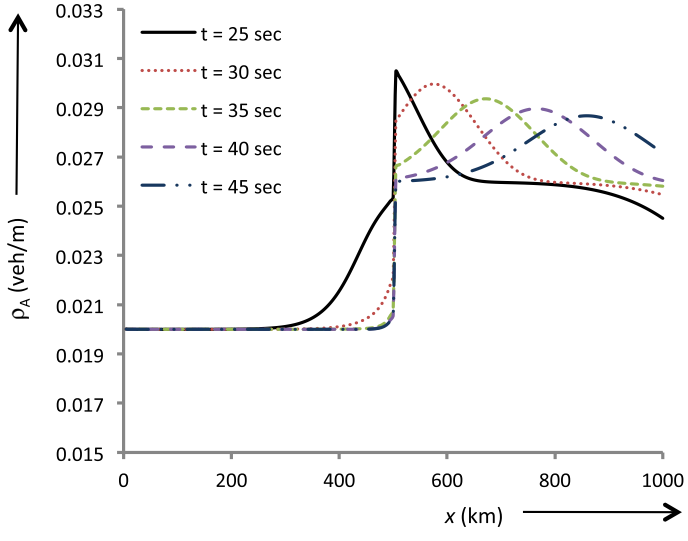

(a)

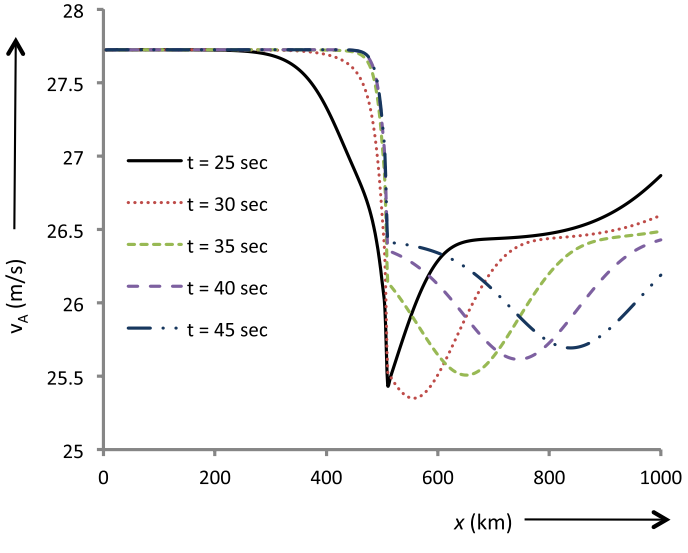

(b)

Fig. 7. (Color online) Evolution of traffic characteristics for four-section model: late time effect. (a) and (c) represent the density profile on road A and B, respectively while (b) and (d) show the velocity profile on road A and B, respectively.

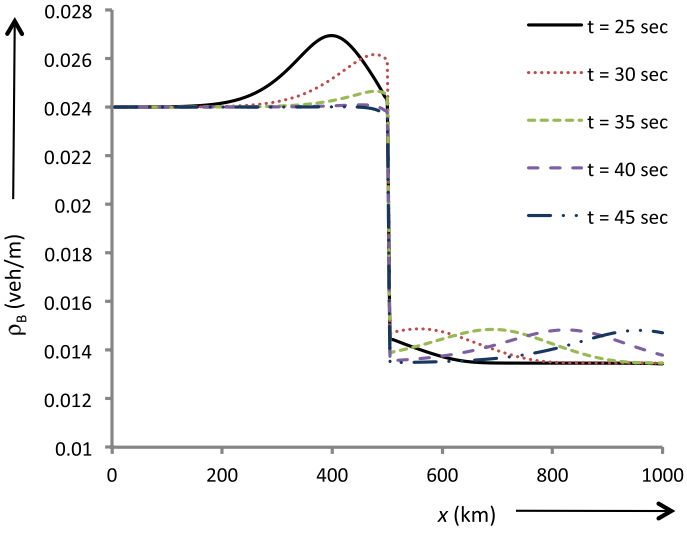

(c)

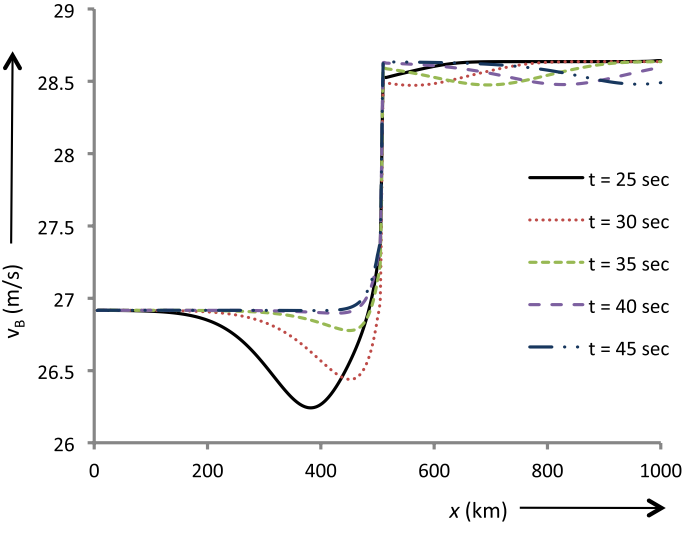

(d)

Fig. 7. (*Continued*)

section 3 continues to travel onto section 4, which results an increase in density on road A at the junction. This was expected because the initial conditions on each road are relatively close and 80% of traffic from section 1 and 60% of the traffic from section 3 at the interchange will move to form the traffic flow onto section 2. The high density traffic on section 2 sees lower density ahead and begins to speed up. As time passes, this behavior continues and the size of the high density region on section 2

increases. Likewise, it is expected that road B will realize a decrease in density at the junction. The same effect can be easily seen on road B in Fig. 6(c). The decrease in density allows for the traffic to speed up and display traffic characteristics that are very similar to the two section simulation. Figure 7 illustrates the late time behavior of traffic density and velocity on both the roads. It is clear from the figure that the wave profiles on sections 2 and 4 for the late time are similar to the profile that was present on the sections 1 and 3 for early time. At $t = 45$ s, Fig. 7 illustrates that the input density on both the roads eventually passes completely through the junction.

It is clear from the numerical simulation on hypothetical test cases of two-section and four-section that the proposed methodology works well in both the situations. But, due to the assumption of unidirectional flow, we need to further extend the model for general highway interchange situations. So, it may be reasonable to conclude that the new junction model can provide an easy and accurate description of traffic flow on networks and results obtained are consistent with the spectrum of nonlinear dynamic properties reported in the literature.

4. Conclusions

In traffic flow, in spite of its complexity to model traffic flow on network, many different robust and powerful theories are presented in the last decade, but most of these approaches are complex and not effective in the case of modeling traffic flow for developing countries like India where most of the junction are congested and extension of road lanes are not possible. In this paper, to model traffic flow network a new section approach, based on the anisotropic continuum model via boundary conditions is introduced. In order to show remarkable insights of our approach, some simulation have been carried out on a two section one lane highway with an entrance ramp and an exit ramp and four section road network comprised of two one lane roads. Contrary to existing models, the specificity of our new approach is not only its ability to describe effectively traffic dynamics in road networks, but also its simplicity to implement and to operate. Furthermore, thanks to its computational efficiency, the model is appropriate to operate in real-time, as required by any traffic management system. The traffic simulations show this method to be extremely effective in order to reduce the number sensors used by civil engineers for traffic flow prediction.

In order to validate the model further investigations like comparison with the empirical data should be carried out. As part of future research it would be interesting to extend this section approach to heterogeneous traffic i.e. with multiple vehicle types. To optimize and stabilize traffic flow, self-control strategies with the help of traffic lights will also be studied.

References

1. M. Bando, K. Hasebe, A. Nakayama, A. Shibata and Y. Sugiyama, *Phys. Rev. E* **51**, 1035 (1995).

2. R. Jiang, Q. S. Wu and Z. J. Zhu, *Phys. Rev. E* **64**, 017101 (2001).
3. M. J. Lighthill and G. B. Whitham, *Proc. R. Soc. Lond. A* **229**, 317 (1955).
4. H. J. Payne, *Mathematical Models of Public Systems*, ed. G. A. Bekey, *Simulation Councils Proceedings Series*, Vol. 1 (Simulation Councils, 1971), pp. 51−60.
5. P. I. Richards, *Oper. Res.* **4**, 42 (1956).
6. B. S. Kerner and P. Konhäuser, *Phys. Rev. E* **48**, 2335 (1993).
7. A. Aw and M. Rascle, *SIAM J. Appl. Math.* **60**, 916 (2000).
8. P. Berg, A. Mason and A. Woods, *Phys. Rev. E* **61**, 1056 (2000).
9. A. K. Gupta and V. K. Katiyar, *J. Phys. A* **38**, 4069 (2005).
10. A. K. Gupta and V. K. Katiyar, *Physica A* **37**, 1674 (2006).
11. R. Jiang, Q. S. Wu and Z. Zhu, *Transp. Res. B* **36**, 405 (2002).
12. H. M. Zhang, *Transp. Res. B* **36**, 275 (2002).
13. R. Sipahi, F. M. Atay and S. I. Niculescu, *SIAM J. Appl. Math.* **68**, 738 (2007).
14. A. Kotsialos, M. Papageorgiou, C. Diakaki, Y. Pavlis and F. Middelham, *IEEE Trans. Intell. Transp. Syst.* **3**, 282 (2002).
15. J. McCrea and S. Moutari, *Eur. J. Oper. Res.* **207**, 676 (2010).
16. D. Helbing, *Phys. Rev. E* **53**, 2366 (1996).
17. C. F. Daganzo, *Transp. Res. B* **29**, 277 (1995).
18. H. Holden and N. H. Risebro, *SIAM J. Math. Anal.* **26**, 999 (1995).
19. M. Herty and A. Klar, *SIAM J. Sci. Comput.* **25**, 1066 (2003).
20. G. Coclite, M. Garavello and B. Piccoli, *SIAM J. Math. Anal.* **36**, 1862 (2005).
21. M. Herty, C. Kirchner and S. Moutari, *Commun. Math. Sci.* **4**, 591 (2006).
22. M. Herty, S. Moutari and M. Rascle, *Netw. Heterog. Media* **1**, 275 (2006).
23. R. Junevičius and M. Bogdevičius, *Transport* **24**, 333 (2009).
24. G. A. Mendes, L. R. Da Silva and H. J. Herrmann, *Physica A* **391**, 362 (2012).